

## A simplified theory of adaptive bone elastic beam buckling

Salah Ramtani<sup>\*1</sup>, Hamza Bennaceur<sup>2a</sup> and Toufik Outtas<sup>2b</sup>

<sup>1</sup>Laboratoire CSPBAT-LBPS UMR 7244 CNRS Université Paris-Nord, Institut Galilée, 99 avenue J.B. Clément, 93430 Villetaneuse, France

<sup>2</sup>Laboratoire Mécanique des Structures et Matériaux Université de Batna, Département de Mécanique, Faculté de technologie, Avenue Chahid Boukhrouf 05000, Batna, Algeria

(Received February 12, 2014, Revised September 24, 2014, Accepted September 30, 2014)

**Abstract.** The usual assumption that the increase of fractures in aging bone is due entirely to lower bone density is taken back with respect to the possibility that aging bone fractures result from a loss of stability, or buckling, in the structure of the bone lattice. Buckling is an instability mode that becomes likely in end-loaded structures when they become too slender and lose lateral support. The relative importance of bone density and architecture in etiology bone fractures are poorly understood and the need for improved mechanistic understanding of bone failure is at the core of important clinical problems such as osteoporosis, as well as basic biological issues such as bone formation and adaptation. These observations motivated the present work in which simplified adaptive-beam buckling model is formulated within the context of the adaptive elasticity (Cowin and Hegedus 1976, Hegedus and Cowin 1976). Our results indicate that bone loss activation process leads systematically to the apparition of new elastic instabilities that can conduct to bone-buckling mechanism of fracture.

**Keywords:** Adaptive elasticity; bone remodeling; beam buckling theory

---

### 1. Introduction

What is well known is that bone modeling/remodeling and architectural changes in our skeleton occur with age and are exaggerated in patients with post-menopausal osteoporosis who suffer from spine fractures. Osteoporosis, characterized as loss of bone mass with deterioration of microstructure and material properties, is known as a growing public health problem (Bell 1967, Kanis *et al.* 2008, Ionovici *et al.* 2009). For example, Paget's disease is known as a chronic focal abnormality in bone turnover. This disease causes an increased and irregular formation of bone as bone cells become uncontrollable. Over a period of time, the deformed new bone becomes larger and weaker, and develops more blood vessels than normal bones. Unlike normal bone, the structure is irregular, which makes it weaker and therefore prone to fracture even from a minor injury (Selby 2002). Three abnormalities that can account for skeletal fragility disproportional to the degree of bone loss have been described (Hasegawa *et al.* 1995, Recker 1995): (a) *a loss of*

---

\*Corresponding author, Professor, E-mail: [ramtani@univ-paris13.fr](mailto:ramtani@univ-paris13.fr)

<sup>a</sup>Ph.D. Student

<sup>b</sup>Professor

*trabecular connectivity such that vertical weight-bearing bars lose their cross attachments with each other, thus becoming susceptible to buckling; (b) an inefficient and prolonged micro damage repair due to periods of pause in the formation phase of remodeling; and (c) an accumulation of unpaired micro damage in unremodeled bone tissue in the central part of trabeculae due to reduced osteon wall thickness coupled with the maintenance of trabecular thickness.*

Müller *et al.* (1998) measured samples of bovine tibiae and whale spine to investigate the influence of bone structure type on the failure mechanism; and they found that, in the whale spine's rod like type of architecture, structural failure consisted of the initial buckling and bending of structural elements followed by the collapse of the overloaded trabeculae. Aging and osteoporosis are known to cause thinning cortices, expansion of outer diameter and loss of internal trabecular support which may lead to local buckling. Lee *et al.* (2005, 2009, 2012), for example, have analyzed eight cross-section models of the femoral neck cortex using dimensions from studies of hip fracture cases and non-fractured controls. Sections were selected to span a range of cortical slenderness based on the buckling ratio; i.e., *maximum outer radius from the center of mass divided by the mean wall thickness*. Potential for local instability was investigated using finite strip models, a specialized variant of the finite element method, of each cross-section and determined the elastic local buckling stress. Their analyses performed under pure compression (Lee *et al.* 2005) suggested that geometries seen in fracture cases are less stable than those in controls and concluded simple constructs to estimate cortical instability such as the buckling ratio may have some value but may not be sufficiently accurate for predictive use whereas more realistic analyses generated in a combination of bending and compression should better simulate the fall conditions producing hip fracture (Lee *et al.* 2009, 2012). It has been hypothesized that the femoral neck of young subjects are more prone to fracture by yielding, whereas those of elderly subjects are more susceptible to fracture initiated by local buckling (Lee *et al.* 2012).

Hydraulic and buckling theories are two accepted mechanisms of the orbital blowout fracture which have been investigated from a clinical, experimental, and theoretical stand point (Warwar *et al.* 2000). These are incomplete fractures where only part of the bone gave way.

Computational analysis using the finite-element method was conducted by Goto *et al.* (2003) in order to compare changes in the coronal and the transverse planes of idiopathic thoracic scoliosis with changes produced in a finite-element buckling model, and to investigate the influence of bone modeling on the buckling spine. As a result, they suggested that scoliotic changes in the spinal column triggered by the buckling phenomenon are counteracted by bone formation, but worsened by bone resorption. The authors hypothesized that scoliosis progressed with resorption of loaded bone.

Even though the reality of many bone fractures mechanisms are complex, what is well argued is that (Parker 2006): (a) bone loss makes the trabeculae longer and more slender, (b) bone turnover introduces physical defects, in terms of resorption pits, (c) in younger trabecular bone, strength-initiated failure dominates, in which the stress overcomes the strength of the bone tissue, (d) in older bone, stability-initiated failure dominates because of the instability of the individual trabeculae which is prone to inelastic buckling at stresses far less than expected for strength-based failure. The need for improved mechanistic understanding of cancellous bone failure is at the core of important clinical problems such as osteoporosis, as well as basic biological issues such as bone formation and adaptation. With respect to known investigations, there is a great need for a theoretical framework that provides insight into the bending–buckling process coupled to bone adaptation which accounts for many fracture mechanisms. As a first step in this direction, we have taken back the previous theory due to Ramtani and Abdi (2005) and stated the particular case of

adaptive Euler-Bernoulli beam hypothesis which has been numerically investigated using a finite difference method. Based on both theoretical and computational analysis, this study intends globally to establish a better knowledge about bone fractures and, in particular to evaluate the influence of the bone adaptation upon the buckling of micro structural bone-beam elements. In this contribution, among other results, we indicate that the activation of bone loss process leads systematically to the apparition of new elastic instabilities that can conduct to local bone-buckling mechanism of fracture localized at the trabeculae scale.

## 2. Theoretical formulation

The present work is conducted within the context of the theory of adaptive elasticity due to Cowin and Hegedus (1976) as a model for the physiological process of bone adaptation and specialized to the case of small strains in isothermal processes (Hegedus and Cowin 1976) will now be summarized. Let  $\rho$  be the bulk density of the porous bone material expressed as

$$\rho = \gamma(\xi_0 + e) \quad (1)$$

where  $e = \xi - \xi_0$  is the measure of the change in solid phase volume fraction from a reference volume fraction  $\xi_0$ ,  $\xi$  is the solid phase volume fraction of the reference unstrained state and  $\gamma$  is the density of the material that composes the matrix structure assumed to be always constant.

The constitutive equation for the *Cauchy* stress is

$$T_{ij} = \left\{ \xi_0 C_{ijkl}^0 + e C_{ijkl}^1 \right\} E_{kl} \quad (2)$$

where  $C_{ijkl}^0$ ,  $C_{ijkl}^1$  are constants tensors representing the elastic properties of the adaptive material, and  $E_{ij}$  is the linearized strain tensor.

The modified Hooke's law from which the proportionality between the Cauchy stress and the linearized strain components is dependent upon the volume fraction of the material present  $e$ , can be written as

$$T_{ij} = \xi_0 T_{ij}^0 + e T_{ij}^1 \quad (3)$$

### 2.1 Initially stressed adaptive elastic beam

#### 2.1.1 General theory formulation

In this section we apply simplified Timoshenko beam theory subjected to an initial stress  $\tau_{\alpha\beta}^0$ . For our purposes, we neglect body forces, and write local equilibrium equations as

$$\sigma_{ij,i} = 0 \quad (4)$$

where  $i, j = x, y, z$  and summations are to be carried out for repeated Greek subscripts only.

One can first write both the local stress partition for the initially pre-stressed beam

$$\left\{ \begin{array}{l} \sigma_{xx} = \xi_0 T_{xx}^0 + \bar{e} T_{xx}^1 + \sigma(x) z \frac{d\psi(x)}{dx}, \quad \sigma_{yx} = \xi_0 T_{yx}^0 + \bar{e} T_{yx}^1, \\ \sigma_{zx} = \xi_0 T_{zx}^0 + \bar{e} T_{zx}^1, \quad \sigma_{xz} = \xi_0 T_{xz}^0 + \bar{e} T_{xz}^1 + \sigma(x) \frac{dw(x)}{dx} \\ \sigma_{yz} = \xi_0 T_{yz}^0 + \bar{e} T_{yz}^1, \quad \sigma_{zz} = \xi_0 T_{zz}^0 + \bar{e} T_{zz}^1 \end{array} \right. \quad (5)$$

and the bone density resultant over the beam's cross-section  $\Sigma_0$

$$\bar{e}(x, t) = \int_{\Sigma_0} e(x, y, z, t) dydz \quad (6)$$

According to the classical one dimensional *Timoshenko* beam theory, incremental displacements measured from the initially stressed equilibrium configuration are stated as

$$u_x = z\psi(x), \quad u_z = w(x) \quad (7)$$

whereas the incremental strain resultants are defined by the following expressions

$$\left\{ \begin{array}{l} m_{xx} = \frac{1}{I_{oy}} \int_{\Sigma_0} z \varepsilon_{xx} dydz \\ q_x = \frac{2}{S_0} \int_{\Sigma_0} \varepsilon_{xz} dydz \end{array} \right. \quad (8)$$

where  $S_0 = bh$ , with  $h$  and  $b$  as the height and width of the rectangular cross-section area of the beam.

In the subsequent development, it will be convenient to define the following adaptive beam stress-resultants

$$\left\{ \begin{array}{l} M(\bar{e}) = \int_{\Sigma_0} z (\xi_0 T_{xx}^0 + \bar{e} T_{xx}^1) dydz = \xi_0 M^0 + \bar{e} M^1 \\ Q(\bar{e}) = \int_{\Sigma_0} (\xi_0 T_{xz}^0 + \bar{e} T_{xz}^1) dydz = \xi_0 Q^0 + \bar{e} Q^1 \end{array} \right. \quad (9)$$

The combination of the Eqs. (8) and (9) leads to the pertinent adaptive-beam resultant stress-strain relation

$$\left\{ \begin{array}{l} M^r(\bar{e}, t) = E^r I_{oy} \left( \frac{d\psi(x)}{dx} \right) \\ Q^r(\bar{e}, t) = k^2 G^r S_0 \left( \psi(x) + \frac{dw(x)}{dx} \right) \end{array} \right. \quad r = 0, 1 \quad (10)$$

where  $S_0$  and  $k^2$  are respectively the cross-sectional area and the ‘‘shear correction factor’’ to compensate for the error in assuming a constant shear strain or stress through the beam thickness (Vinson 1989).

Next we set  $j = x$  in Eq. (4), and multiply each term by  $z$ . Subsequent application of the

operation  $\int_{\Sigma_0} \dots dydz$  to each term results in

$$\int_{\Sigma_0} z \frac{d(\xi_0 T_{xx}^0 + \bar{e} T_{xx}^1)}{dx} dydz + \frac{d}{dx} \left( \sigma(x) \frac{d\psi(x)}{dx} \right) \int_{S_0} z^2 dydz + \int_{\Sigma_0} z \left( \frac{\partial(\xi_0 T_{yx}^0 + \bar{e} T_{yx}^1)}{\partial y} + \frac{\partial(\xi_0 T_{zx}^0 + \bar{e} T_{zx}^1)}{\partial z} \right) dydz = 0 \quad (11)$$

With the aid of (9), the first integral in (11) can be reduced as

$$\int_{\Sigma_0} z \frac{d(\xi_0 T_{xx}^0 + \bar{e} T_{xx}^1)}{dx} dydz = \frac{d}{dx} (\xi_0 M^0 + \bar{e} M^1) \quad (12)$$

The third integral in (11) can be reduced by Green's theorem in the  $y - z$  plane,

$$\int_{\Sigma_0} z \left( \frac{\partial(\xi_0 T_{yx}^0 + \bar{e} T_{yx}^1)}{\partial y} + \frac{\partial(\xi_0 T_{zx}^0 + \bar{e} T_{zx}^1)}{\partial z} \right) dydz = \xi_0 \oint_C z (T_{yx}^0 n_y + T_{zx}^0 n_z) ds + \bar{e} \oint_C z (T_{yx}^1 n_y + T_{zx}^1 n_z) ds - \int_{\Sigma_0} (\xi_0 T_{zx}^0 + \bar{e} T_{zx}^1) dydz \quad (13)$$

On the lateral surface of the beam (i.e., on  $C$ ) we have  $n_x=0$ , either exactly or approximately. In this case,  $t_x^r = T_{yx}^r n_y + T_{zx}^r n_z = 0$  on  $C$  for  $r=0,1$ . Thus, Eq. (13) becomes

$$\int_{\Sigma_0} z \left( \frac{\partial(\xi_0 T_{yx}^0 + \bar{e} T_{yx}^1)}{\partial y} + \frac{\partial(\xi_0 T_{zx}^0 + \bar{e} T_{zx}^1)}{\partial z} \right) dydz = -(\xi_0 Q^0 + \bar{e} Q^1) \quad (14)$$

Upon utilization of (12) and (14), Eq. (11) assumes the form

$$\frac{d}{dx} (\xi_0 M^0 + \bar{e} M^1) + I_{Oy} \frac{d}{dx} \left( \sigma(x) \frac{d\psi(x)}{dx} \right) - (\xi_0 Q^0 + \bar{e} Q^1) = 0 \quad (15)$$

and in view of the first equation of (9), this equation can be written as

$$\frac{d}{dx} \left( \xi_0 M^0 \left( 1 + \frac{\sigma(x)}{\xi_0 E^0} \right) + \bar{e} M^1 \right) - (\xi_0 Q^0 + \bar{e} Q^1) = 0 \quad (16)$$

For most applications,  $\frac{\sigma(x)}{\xi_0 E^0} \ll 1$ , and therefore

$$\frac{d}{dx} (\xi_0 M^0 + \bar{e} M^1) - (\xi_0 Q^0 + \bar{e} Q^1) = 0 \quad (17)$$

Next, we set  $j=z$  in (4) and apply the operator  $\int_{\Sigma_0} \dots dydz$  to each. With the aid of (5), we

obtain

$$\int_{\Sigma_0} \frac{d(\xi_0 T_{xz}^0 + \bar{e} T_{xz}^1)}{dx} dydz + \frac{d}{dx} \left( \sigma(x) \frac{dw(x)}{dx} \right) \int_{\Sigma_0} dydz + \int_{\Sigma_0} \left( \frac{\partial(\xi_0 T_{yz}^0 + \bar{e} T_{yz}^1)}{\partial y} + \frac{\partial(\xi_0 T_{zz}^0 + \bar{e} T_{zz}^1)}{\partial z} \right) dydz = 0 \quad (18)$$

and in view of (9) we obtain,

$$\frac{d}{dx} (\xi_0 Q^0 + \bar{e} Q^1) + S_o \frac{d}{dx} \left( \sigma(x) \frac{dw(x)}{dx} \right) + \int_{\Sigma_0} \left( \frac{\partial(\xi_0 T_{yz}^0 + \bar{e} T_{yz}^1)}{\partial y} + \frac{\partial(\xi_0 T_{zz}^0 + \bar{e} T_{zz}^1)}{\partial z} \right) dydz = 0 \quad (19)$$

The third term in (18) can be reduced by application of Green's theorem. We have,

$$\int_{\Sigma_0} \left( \frac{\partial(\xi_0 T_{yz}^0 + \bar{e} T_{yz}^1)}{\partial y} + \frac{\partial(\xi_0 T_{zz}^0 + \bar{e} T_{zz}^1)}{\partial z} \right) dydz = \oint_C \xi_0 (T_{yz}^0 n_y + T_{zz}^0 n_z) ds + \oint_C \bar{e} (T_{yz}^1 n_y + T_{zz}^1 n_z) ds \quad (20)$$

$$= \oint_C (\xi_0 t_z^0 + \bar{e} t_z^1) ds = \xi_0 p^0(x) + \bar{e} p^1(x)$$

and because on the beam lateral surface  $t_z^r = (T_{yz}^r n_y + T_{zz}^r n_z)$ ,  $r = 0, 1$ , either exactly or approximately.  $p(x) = \xi_0 p^0(x) + \bar{e} p^1(x)$ , corresponds to the distributed transverse applied force acting on the beam. Finally, we obtain the following equation,

$$\frac{d}{dx} \left( \xi_0 Q^0 + \bar{e} Q^1 + S_o \sigma(x) \frac{dw(x)}{dx} \right) + \xi_0 p^0(x) + \bar{e} p^1(x) = 0 \quad (21)$$

The rate of change in the resultant volume fraction  $\bar{e}(x, t)$  of the material present is now expressed in terms of resultant strains as

$$\frac{d}{dx} \bar{e}(x, t) = a_0 + a_1 \bar{e} + a_2 \bar{e}^2 + (A_{xx}^0 + \bar{e} A_{xx}^1) m_{xx} + (A_{xz}^0 + \bar{e} A_{xz}^1) q_x \quad (22)$$

An important prediction of the theory of buckling of adaptive elastic bone-beam can be derived following the system of Eqs. (17), (21), (22) and the associated initial and boundary conditions.

### 2.1.2 Euler Bernoulli hypothesis

Trabeculae are known as anastomosing bony spicules in cancellous bone which form a meshwork of intercommunicating spaces that are filled with bone marrow. In some bone of the skull, these internal spaces are enlarged and lined by respiratory epithelium and are contiguous with the nasal cavity. The insertion of these elements could probably affect the boundary conditions, and/or introduce some of viscous damping. However, changing the boundary conditions do not disturb notably the bone adaptation process as well as the apparition of observed

elastic instabilities. As an application of the stated adaptive beam buckling theory, it is proposed to neglect: (a) the effects of shear deformation by setting  $\psi(x) = -\frac{dw(x)}{dx}$ , (b) both the first  $\bar{e}_{,x}$  and second  $\bar{e}_{,xx}$  derivatives of the remodeling variable, and (c) both transverse applied loads  $p^0 \approx 0$ ,  $p^1 \approx 0$ . The governing Eq. (23) for the dimensionless deflection mode  $\bar{w}(\bar{x}) = \frac{w(x)}{L}$  takes the form

$$\left(1 + \eta \frac{\bar{e}}{\xi_0}\right) \frac{d^4 \bar{w}(\bar{x})}{d\bar{x}^4} - \frac{P L^2}{\xi_0 E^0 I_{Oy}} \frac{d^2 \bar{w}(\bar{x})}{d\bar{x}^2} = 0 \quad (23)$$

where  $\bar{x} = \frac{x}{L}$  is the dimensionless length,  $P$  is the applied compressive load,  $\eta = \frac{E^1}{E^0}$  is a material parameter derived as the ratio of the primary  $E^0$  and secondary  $E^1$  elastic modulus.

For commodity reason, let us assume that  $A_{ij}^0 = A_{ij}^1 = A$  which leads to the following bone remodeling law

$$\frac{d}{dt} \bar{e}(\bar{x}, t) = a_0 + a_1 \bar{e} + a_2 \bar{e}^2 - A(1 + \bar{e}) \frac{d^2 \bar{w}(\bar{x})}{d\bar{x}^2} \quad (24)$$

### 3. Results and discussion

It should be remarked that the beam is in a remodeling equilibrium. This means that before insertion the equation (24) reduces to  $a_0 + a_1 \bar{e} + a_2 \bar{e}^2 = 0$  where the initial solid volume fraction  $e_0 = 0.0667$  is one of the dominating roots.

It is well known that boundary conditions have a notable effect on the critical load of slender columns (Saha, 2007). They determine the mode of bending (i.e., buckled shape) and the distance between inflection points on the deflected column.

Our numerical solutions are conducted and illustrated with respect to  $0 < \eta \leq 1$ , the hypothetical data given in table 1 (Cowin and van Buskirk, 1978) and concerns a particular situation of a bone-beam column which is fixed at one end ( $\bar{x} = 0$ ), pinned at the other end ( $\bar{x} = 1$ ) and loaded at the free end by a concentrated compressive force  $\mathbf{P}$  (Fig. 1). The corresponding boundary conditions are as follows:

$$\begin{cases} \bar{w}(\bar{x}) = 0. & \text{and} & \frac{d\bar{w}(\bar{x})}{d\bar{x}} = 0. & \text{at } \bar{x} = 0. \\ \bar{w}(\bar{x}) = 0. & \text{and} & \frac{d^2 \bar{w}(\bar{x})}{d\bar{x}^2} = 0. & \text{at } \bar{x} = 1. \end{cases} \quad (25)$$

Let us consider firstly, the case where the remodeling rate coefficient is  $A=0.5$  and  $\eta=0.1$ . It can be observed that the beam's deflection remains stable during the remodeling process (Fig. 2a) and its associated bone remodeling distribution exhibits a singular node, located at  $\bar{x} = 0.3$ , for which the bone density is constant (Fig. 2b). It is shown that at both left and right sides of this

node, bone resorption (i.e., decreasing bone density) and apposition (i.e., increasing bone density) occur respectively.

Table 1 Hypothetical parameters

Bone remodeling parameters	$a_0(s^{-1})$	$a_1(s^{-1})$	$a_2(s^{-1})$	$A(s^{-1})$	$\gamma(g/cm^3)$	$\zeta_0$
	$10^{-8}$	$2.50 \cdot 10^{-7}$	$1.50 \cdot 10^{-6}$	0.50	0.65	0.892
Geometrical and elastic parameters	$L(mm)$	$b(mm)$	$h(mm)$	$E^0(Pa)$	$\eta$	$n$
	1.00	0.10	0.10	$18.40 \cdot 10^9$	0.10	35

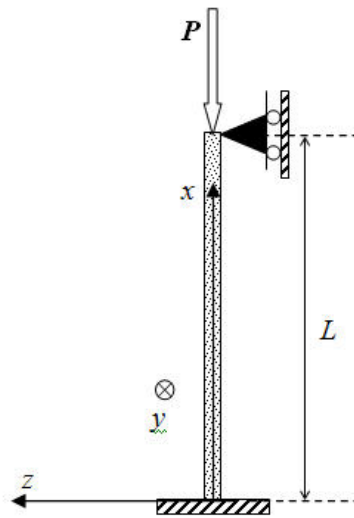


Fig. 1 Beam's column with end axial load

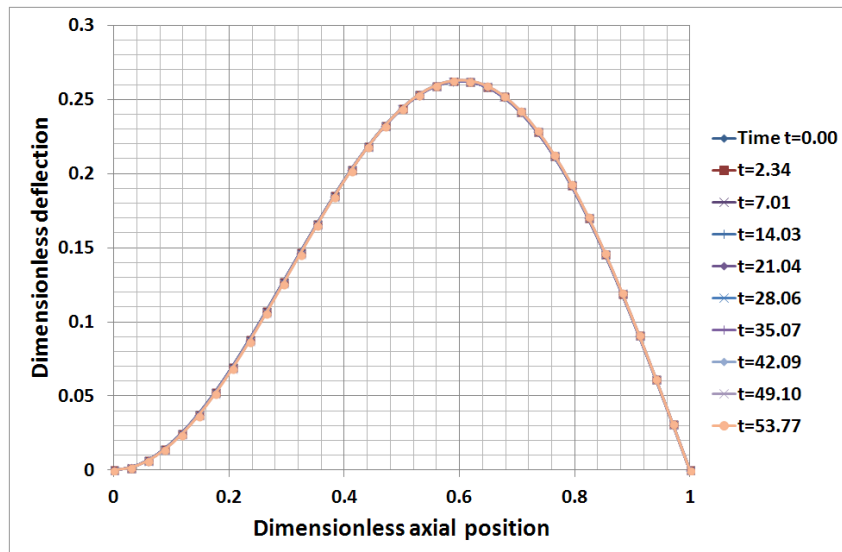


Fig. 2a Beam's deflection  $\bar{w}(\bar{x})$  over the time for  $A=0.5$  and  $\eta=0.1$

*A simplified theory of adaptive bone elastic beam buckling*

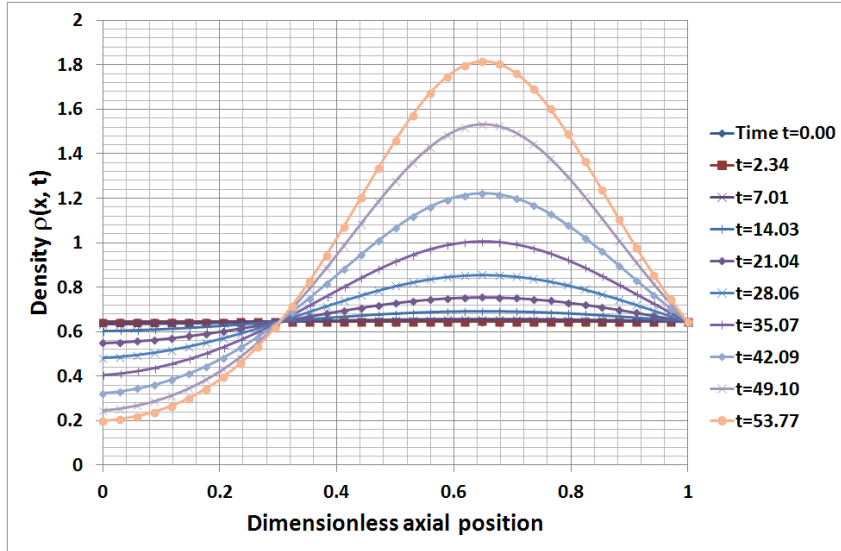


Fig. 2b Bone density ( $g/cm$ ) distribution over the time for  $A=0.5$  and  $\eta=0.1$

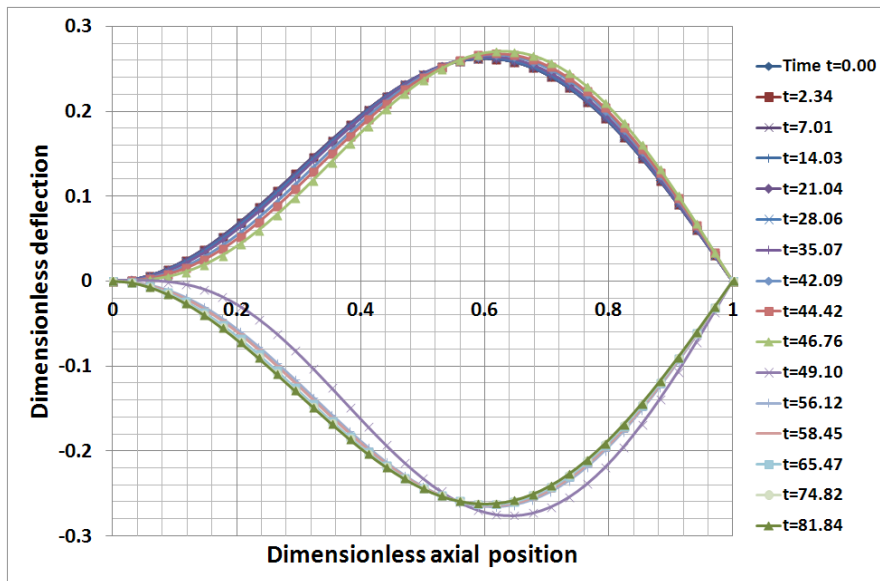


Fig. 3a Beam's deflection  $\bar{w}(\bar{x})$  over the time for  $A=0.5$  and  $\eta=0.85$

Both beam's deflection and density distributions are analyzed (Fig. 3) for the remodeling rate coefficient  $A=0.5$  and  $\eta=0.85$ . In this case, the beam's situation is different because it can be noted that the bone beam starts with a stable positive deflection and at  $t = 46.76$  days, a small shift appears. This shift leads to a change of sign of the beam's deflection at  $t = 49.10$  as well as a light shift with respect to the stabilized situation (Fig. 3a). In Fig. 3b we observe that when the beam's deflection is positive, at the left side of the singular node, also located at  $\bar{x} = 0.3$ , resorption process occurs whereas at the right side the opposite process (i.e., apposition) is in action. Just

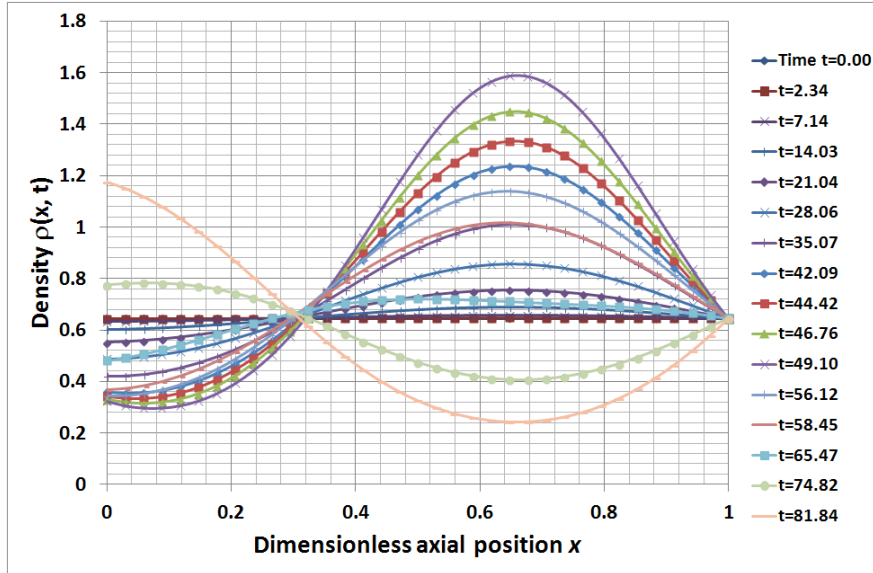


Fig. 3b Bone density ( $g/cm^3$ ) distribution over the time for  $A=0.5$  and  $\eta=0.85$

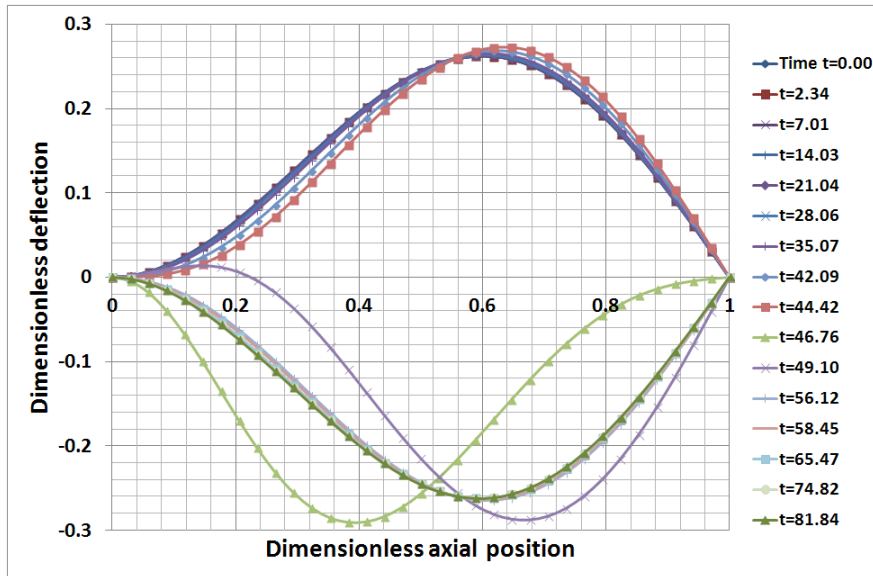


Fig. 4a Beam's deflection  $\bar{w}(\bar{x})$  over the time for  $A=0.5$  and  $\eta=1.0$

after the change of sign of the deflection, the opposite process is in activity on both sides of the singular node.

As a result, one can see that the bone density at the left side is reinforced whereas at the right side the bone density is weakened. At the end of the bone remodeling process this situation is opposite to the preceding case (Fig. 2b).

The same investigations are now renewed for the case  $A=0.5$  and  $\eta=1.0$ . In this case, the

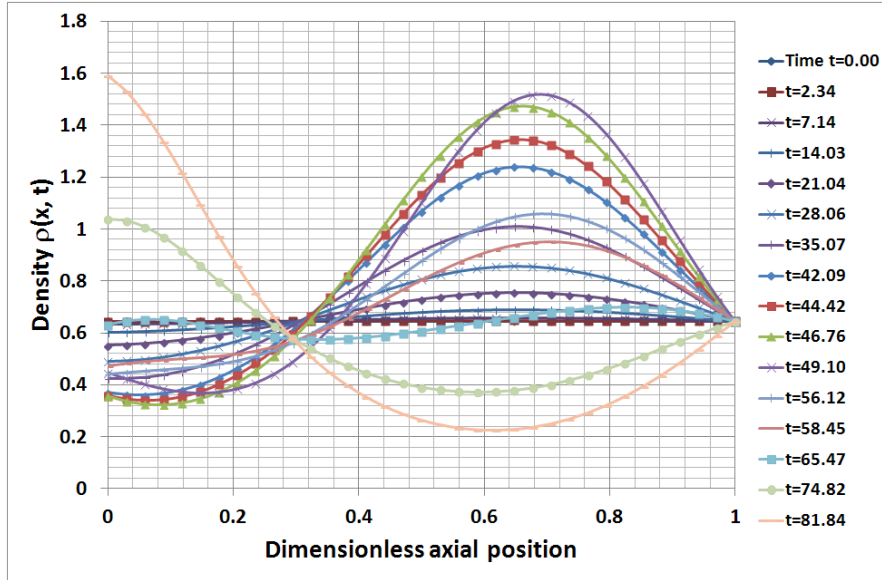


Fig. 4b Bone density ( $g/cm^3$ ) versus position  $\bar{x}$  over the time for over the time for  $A=0.5$ ,  $\eta=1.0$

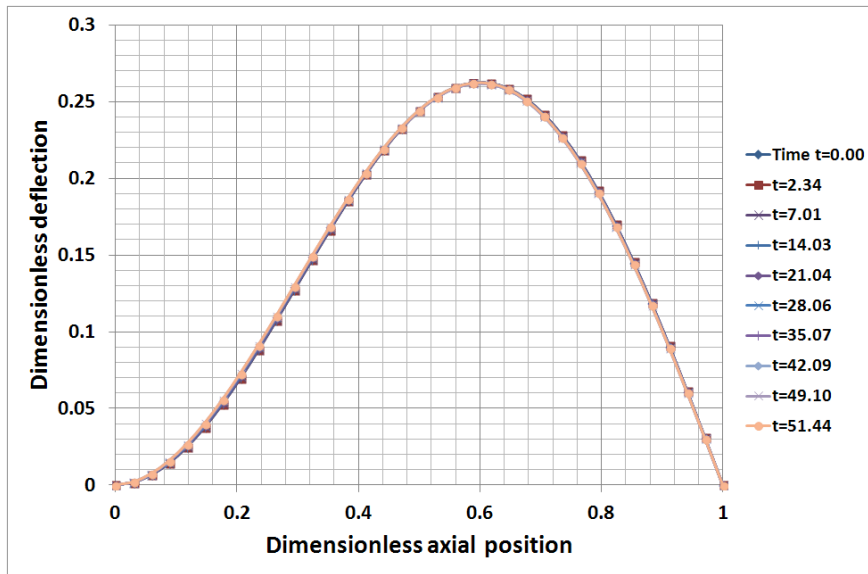


Fig. 5a Beam's deflection  $\bar{w}(\bar{x})$  over the time for  $A=-0.5$ ,  $\eta=1.0$

beam's situation is still different from the preceding case, and it is interesting to note the appearance, at  $t = 46.76$  and  $t = 49.10$  days, of particular instabilities (Fig. 4a). Moreover, the first deflection mode of the beam remains stable despite the complex remodeling process that occurs throughout the beam (Fig. 4a). The density distribution presented in Fig. 4(b) is quite similar to the previous case at its final stage. Our study demonstrates that bone loss is behind the apparition of additional elastic instabilities

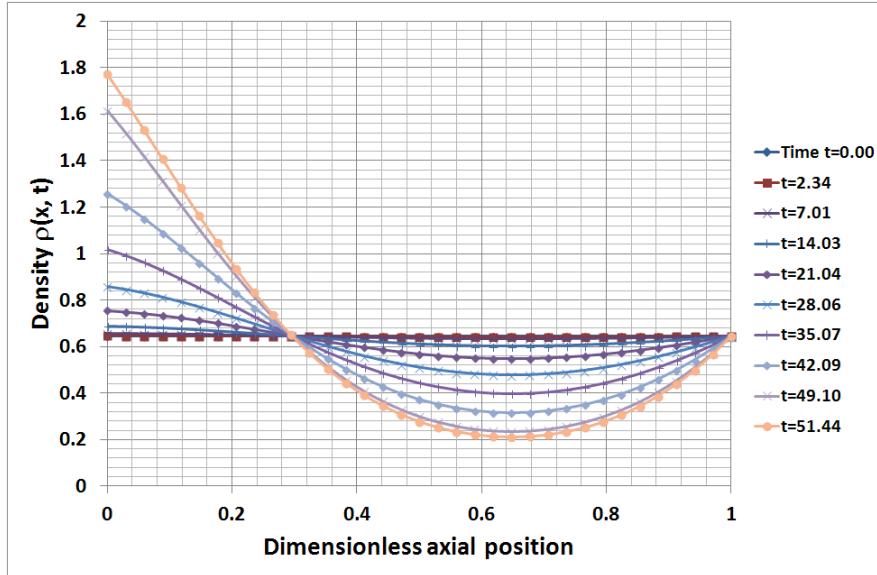


Fig. 5b Bone density ( $g/cm^3$ ) versus position  $\bar{x}$  over the time for  $A=-0.5$ ,  $\eta=1.0$

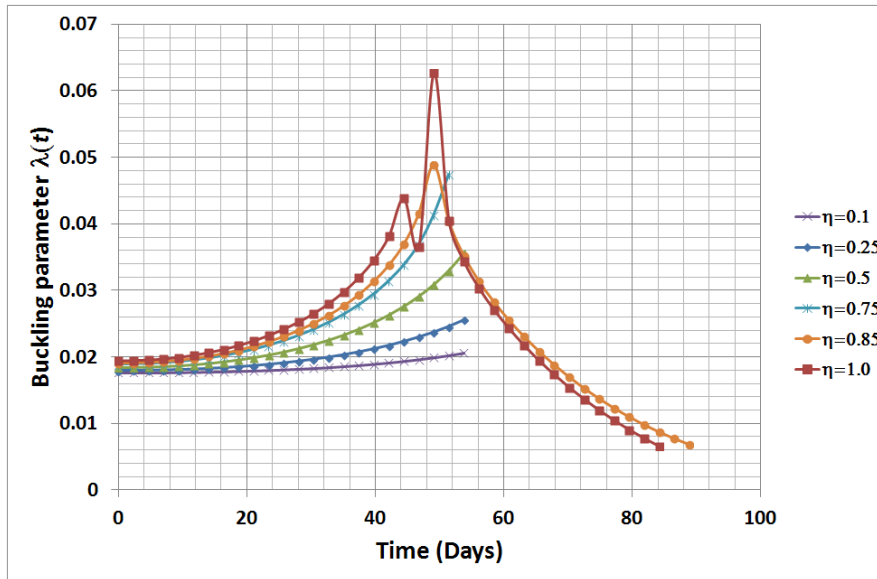


Fig. 6a Buckling parameter versus time for  $A=0.5$

The last case concerns the situation where the remodeling rate coefficient is positive  $A=-0.5$  and  $\eta=1.0$  but remains valid and representative for the other values of  $\eta$  (i.e., 0.10 and 0.85). It can be observed in Fig. 5(a) that the beam's deflection remains stable during the remodeling process and seems to be the same as previous result shown in Fig. 2(a).

As regards the bone density distribution (Fig. 5b), the remodeling process is reversed. One witnesses an important reinforcement activity on the left of the singular node, still located at

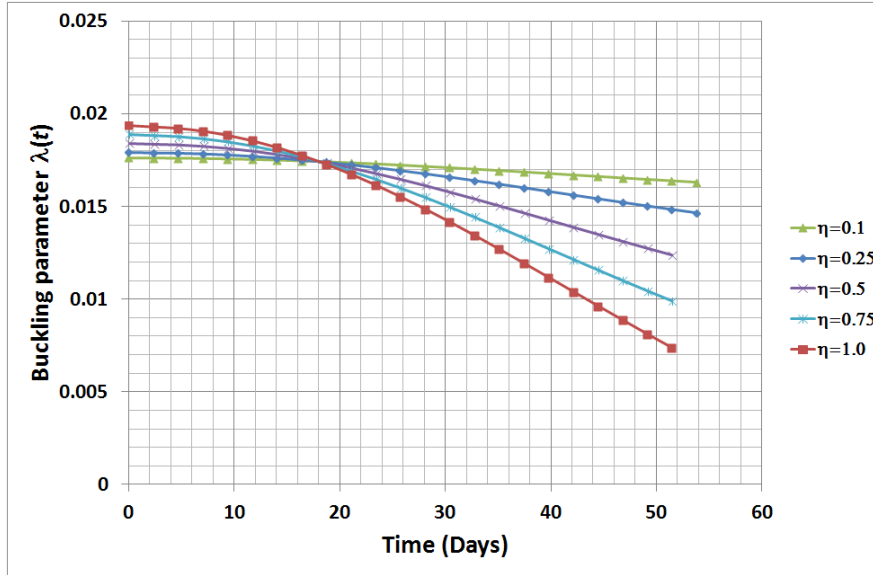


Fig. 6b Buckling parameter versus time for  $A=-0.5$

$\bar{x} = 0.3$ , whereas resorption activity occurs at its right side.

We define the buckling load parameter  $\lambda = \frac{P \Delta x^2}{\xi_0 E^0 I_{Oy}}$  where  $\Delta x$  is the step size of the finite

difference approximation; and as we can see in Fig. 6, its temporal evolution is significantly affected by the variation of the material parameter  $\eta$ . When the remodeling rate coefficient is  $A=0.5$ , the critical load parameter is increasing nonlinearly until reaching a peak value (two peaks for  $\eta=1.0$ ) and then, for particular values of the material parameter  $\eta$ , decreases asymptotically.

The case where is investigated in Fig. 6(b) and it is shown that the buckling load parameter exhibits a decreasing evolution which is accentuated with respect to the increase of the material parameter. It is thus rather easy to establish the link between the peaks values and the elastic instability (intermediate deflection mode (Fig. 4a), change of sign of the mode I of deflection (Fig. 3a)).

#### 4. Conclusions

This study concerns a single trabecula known as anastomosing bony spicules in cancellous bone which form a meshwork of intercommunicating spaces that are filled with bone marrow. In some bone of the skull, these internal spaces are enlarged and lined by respiratory epithelium and are contiguous with the nasal cavity. The insertion of these elements could probably affect the boundary conditions, and/or introduce some of viscous damping.

In our knowledge, this contribution is the first attempt that used adaptive elasticity in order to state a new adaptive-beam (or column) buckling theory at the scale of trabeculae. It is clearly shown that, except for the initial first mode which appears systematically with respect to the stated boundary conditions, the activation of bone loss process, which appears only for  $A>0$ , is behind the

apparition of a new elastic instability that leads to changes in sign of the curvature of the bone-beam's deflection.

For one, it is clearly stated here that from the choice of the bone remodeling rate coefficient  $A$  depends the elastic stability of the bone-column. For another, the authors believe that the number of these elastic instabilities which are potentially implied in the mechanisms of bone fracture, localized at the trabeculae scale, depends strongly upon the material parameter  $\eta$ .

It is evident that both the illustrative character of the example treated here with specific boundary conditions; and the lack of experimental data remains the main limitations of the present contribution. We only are at the beginning of something which is promising but still enough far from the clinical applications. However, this study will provides a new basis for developing appropriate experimental protocols and/or to establish a better knowledge about old bone fractures which is known as prone to inelastic buckling at stresses far less than expected for strength-based failure.

## References

- Bell, G.H. (1967), "Variations in strength of vertebrae with age and their relation to osteoporosis", *Calcified Tiss. Res.*, **1**(1), 75-86.
- Cowin, S.C. and Van Buskirk, W.C. (1978), "Internal bone remodeling induced by a medullary pin", *J. Biomech.*, **11**(5), 269-275.
- Cowin, S.C. and Hegedus, D.M. (1976), "Bone remodeling I : Theory of adaptive elasticity", *J. Elasticity.*, **6**(3), 313-325.
- Frost, H.M. (1964), *Laws of bone structure*, Springfield, MA: Charles C Thomas.
- Goto, M., Kawakami, N., Azegami, H., Matsuyama, Y., Takeuchi, K. and Sasaoka, R. (2003), "Buckling and bone modeling as factors in the development of idiopathic scoliosis", *Spine*, **28**(4), 364-70.
- Hasegawa, K., Turner, C.H., Recker, R.R., Wu, E. and Burr, D.B. (1995), "Elastic properties of osteoporotic bone measured by scanning acoustic microscopy", *Bone*, **16**(1), 85-90.
- Hegedus, D.H. and Cowin, S.C. (1976), "Bone remodeling II: Small strain adaptive elasticity", *J. Elasticity.*, **6**(4), 337-352.
- Ionovici, N., Negru, M., Grecu, D., Vasilescu, M., Mogoanta, L., Bold, A. and Traistaru, R. (2009), "Hypothesis of microfractures by buckling theory of bone's trabeculas from vertebral bodies affected by osteoporosis", *Romanian. J. Morphol. Embryol.*, **50**(1), 79-84.
- Kanis, J.A., McCloskey, E., Johansson, H., Oden, A., Melton, L.J. and Khaltsev, N. (2008), "A reference standard for the description of osteoporosis", *Bone*, **42**(3), 467-475.
- Lee, T., Rammohan, A.V., Chan, A., Chye Tan, V.B., Das De, S. Link, T.M., Eckstein, F. and Schafer, B.W. (2012), "The susceptibility of the femoral neck to fracture: An assessment incorporating the effects of age-remodeling and stress reduction", *J. Biomech.*, **45**(6), 931-937.
- Lee, T., Choi, J.B., Schafer, B.W., Segars, W.P., Eckstein, F., Kuhn, V. and Beck, T.J. (2009), "Assessing the susceptibility to local buckling at the femoral neck cortex to age-related bone loss", *Ann. Biomed. Eng.*, **37**(9), 1910-1920.
- Lee, T.C., Noelke, L., McMahon, G.T., Mulville, J.P. and Taylor, D. (1998), "Functional adaptation in bone", Eds. P. Pedersen and M.P. Bendsoe, *Synthesis in Bio Solid Mechanics*, Kluwer Academic Publishers, Dordrecht.
- Lee, T., Schafer, B.W., Loveridge, N., Reeve, J. and Beck, T.J. (2005), "Finite strip analysis in the assessment of local buckling capacity of the femoral neck", *Meeting of the Orthopedic Research Society*, Washington, DC.
- Müller, R., Gerber, S.C. and Hayes, W.C. (1998), "Micro-compression: a novel method for the non-destructive assessment of bone failure", *J. Biomech.*, **31**, 150-150.

*A simplified theory of adaptive bone elastic beam buckling*

- Parker, A. (2006), "A new look at how aging bones fracture", *Sci. Tech. Rev.*, UCRL-TR-52000-06-9 Distribution Category UC-99 September, 20-21.
- Ramtani, S. and Abdi, M. (2005), "Buckling of adaptive elastic bone-plate: theoretical and numerical investigation", *Biomech. Model. Mechanobiol.*, **3**(4), 200-208.
- Recker, R.R. (2007), "Skeletal fragility and bone quality", *J. Musculoskelet. Neuronal Interact.*, **7**, 54-55.
- Saha, G. and Banu, S. (2007), "Buckling load of beam column for different end conditions using multi-segment integration technique", *ARNP, J. Eng. Appl. Sci.*, **2**(1), 27-32.
- Selby, P.L., Davie, M.W.J., Ralston, S.H. and Stone, M.D. (2002), "Guidelines on the management of Paget's disease of bone", *Bone*, **31**(3), 10-19.
- Vinson, J.R. (1989), "The behavior of thin walled structures-Beams, plates, and shells", Dordrecht etc., Kluwer Academic Publishers.
- Warwar, R.E., Bullock, J.D., Ballal, D.R. and Ballal, R.D. (1999), "Mechanisms of orbital floor fractures: A clinical, experimental, and theoretical study", *Trans. Am. Ophthalmol. Soc.*, **97**, 87-113.

MC